

PAPER • OPEN ACCESS

## Influence of secondary flows on heat transfer from a localized heat source

To cite this article: A. Evgrafova *et al* 2017 *J. Phys.: Conf. Ser.* **899** 022005

View the [article online](#) for updates and enhancements.

### Related content

- [Influence of geometrical parameters on convective flows in non-uniformly heated cylindrical fluid layers](#)  
A. Evgrafova, A. Sukhanovskii, M. Kuchinskii et al.
- [Counter-gradient heat transport by large-scale circulation in two-dimensional turbulent convection](#)  
Wei Qiang, Hui Cao, Weimin Li et al.
- [Secondary convective flows in the rectangular tank with non-uniform heating](#)  
A Teymurazov, A Sukhanovsky, V Batalov et al.

# Influence of secondary flows on heat transfer from a localized heat source

A. Evgrafova<sup>1,2</sup>, A. Sukhanovskii<sup>1</sup>, M. Kuchinskii<sup>2</sup>

<sup>1</sup>Institute of Continuous Media Mechanics, Academ. Korolyov, 1, Perm, 614013, Russia

<sup>2</sup>Perm State University, Bukireva St. 15, Perm, 614990, Russia

E-mail: eav@icmm.ru

**Abstract.** Heat transfer from a localized heat source in a cylindrical fluid layer was studied experimentally. Experiments were performed for fluids with different values of the Prandtl number and for the Rayleigh number from  $10^5$  to  $10^7$ . Particular attention has been paid to investigating the influence of small-scale convective structures in the boundary layer of a basic flow on heat transfer. The dependence of the Nusselt number on the Rayleigh number was obtained by means of temperature measurements. In addition, the mean velocity of convergent flow was estimated. It has been found that changes in the structure and intensity of secondary flows have a weak effect on heat transfer. At the same time, when the Rayleigh number increases, the basic flow velocity exhibits a linear growth.

## 1. Introduction

Natural convection is the primary mechanism of heat transfer in many geophysical and technological processes. In this paper we focus on the case when the heated area is localized. Unlike the Rayleigh-Benard convection in the enclosed volumes heated from below and cooled from above, which was extensively studied experimentally and numerically (see references in [1]), convection from localized heat sources obtained less attention. Convective flows from a localized heat source in two-dimensional formulation for the moderate values of the Rayleigh number (up to  $10^6$ ) were studied in [2] and for turbulent regimes in [3], where  $Ra$  varied from  $10^8$  to  $10^{12}$ . Three-dimensional simulation of convection due to a discrete heat source was carried out in [4] but only for  $Ra$  less than  $10^6$ . However the appearance of secondary flows has not been investigated in these works.

When the size of the heater exceeds the fluid depth in the temperature boundary layer, the secondary convective structures in the form of horizontal rolls are generated [5]. Horizontal rolls formation over the hot plate in the case of forced convection in a rectangular channel was studied in [6,7,8] and in the case of thermal convection in a rectangular vessel in [9]. These studies showed that convective rolls substantially enhance heat transfer due to intensive mixing in the boundary layer.

Important problem is the influence of the secondary flow structure on heat transfer. In [9], it was found that a transition from longitudinal to transverse rolls leads to relatively weak changes in the local Nusselt number (less than 20%) for the same values of the Rayleigh number. Increasing of  $Ra$  leads to the remarkable change in the secondary flow structure [5]. The aim of this study is to realize how heat transfer depends on the structure of secondary flows.



## 2. Experimental setup

Cylindrical vessel of diameter  $D = 300$  mm, and height  $L = 40$  mm was used as an experimental setup. The schematic diagram of the setup is given in figure 1 a. The sides and bottom of the vessel are made of plexiglas with a thickness 3 mm and 20 mm, respectively. There was no cover or additional heat insulation on the sidewalls. The heater is a brass cylindrical plate mounted flush with the bottom. The diameter of the plate is  $d = 100$  mm, and its thickness is 10 mm. The brass plate is heated by an electrical coil placed on the lower side of the disc. There are two ways of controlling heating which leads to different boundary conditions. It can be a constant temperature or a constant heat flux. In the experiments we changed the heating intensity by varying the heat flux. For each experiment the heat flux was fixed and controlled. The heater temperature was measured by an embedded thermocouple. Silicon oils with different values of Prandtl number, PMS-20, PMS-10 and PMS-5 (20, 10 and 5 cSt at  $T = 25$  °C), were used as working fluids. In all experiments, the depth of the fluid layer was  $h = 30$  mm, and the surface of the fluid was always open. Cooling of the fluid is provided mainly by the heat exchange with the surrounding air on the free surface and some heat losses through sidewalls. The temperature of the fluids was measured by a horizontal row of 12 copperconstantan thermocouples. The location of the thermocouples is also shown in figure 1. The coordinate origin is at the center of the bottom. The thermocouples can be moved through the whole layer depth with a step of 1 mm by a motorized translation stage. The data from the thermocouples were obtained by an Agilent 34970A data acquisition switch unit with a 16-channel multiplexer module 34902A. Temperature was measured in the central vertical cross-section above the heating area. To estimate the mean temperature of the fluid, one thermocouple measured temperature inside the fluid layer at mid-height ( $z = 15$  mm), near the periphery (about 3 cm from the sidewall).

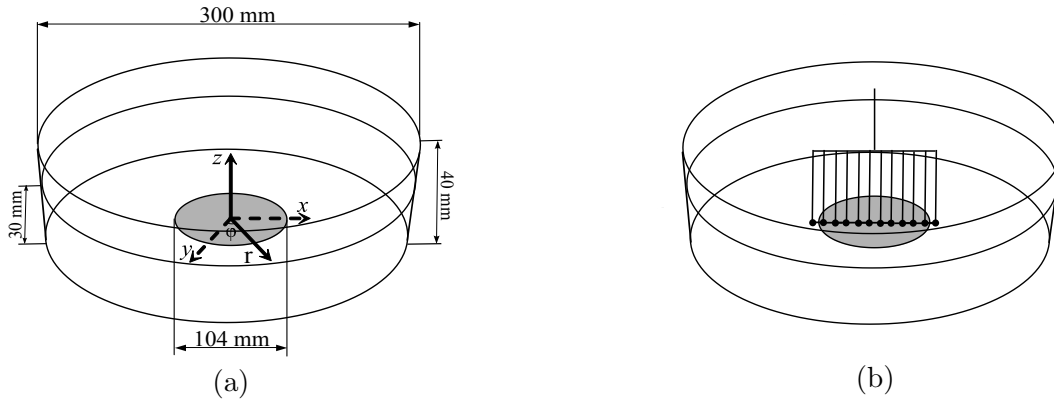


**Figure 1.** Experimental setup, dimensions and location of the coordinate system.

As non-dimensional parameters, we used Prandtl number  $Pr$  and Rayleigh number  $Ra$ :

$$Pr = \frac{\nu}{\chi} \quad (1)$$

$$Ra = \frac{g\beta h^3 \Delta T}{\nu\chi} \quad (2)$$

where  $g$  is the gravitational acceleration,  $h$  is the layer depth,  $\beta$  is the coefficient of thermal expansion,  $\Delta T$  is the temperature difference between the temperature of the heater and the environment temperature,  $\nu$  is the coefficient of kinematic viscosity, and  $\chi$  is the thermal diffusivity.

Heat transfer was characterized by the Nusselt number defined as

$$Nu = \frac{q}{q_\lambda} \quad (3)$$

where  $q_\lambda$  is heat flux due to conduction, and  $q$  is overall heat flux. The heat fluxes  $q$  and  $q_\lambda$  were calculated as

$$q = \frac{P}{S}; q_\lambda = \lambda \frac{T_h - T_s}{h} \quad (4)$$

where  $P$  is the power of the heater,  $S$  is the heater surface area,  $T_h$  is the temperature of the heater, and  $T_s$  is the temperature of the fluid surface. The temperature of the fluid surface  $T_s$  was received by the following way. The row of thermocouples measured the temperature of fluid above the heater consistently at  $z = 28, 29$  and  $30$  mm. The time of measurements was about 1000 seconds for each height. Then, the temperature was averaged over time and space in this thin near-surface layer, and the resulting temperature ( $T_s$ ) was used to calculate the heat flux  $q_\lambda$ . Here, we neglect heat losses through the bottom and side walls.

The temperature  $T_s$  is the mean value of temperature along the thermocouple row, which is placed in the central part of the vessel above the heater. Parallel with the experiment, temperature fields of a fluid surface were obtained by a thermal imager Fluke Ti32 system for different regimes. Temperature sensitivity of the Fluke Ti32 is high (about  $0.05^\circ C$ ), but temperature measurement accuracy is  $\pm 2^\circ C$  and it needs to be calibrated for every regime. Therefore it was used only for getting information about temperature distribution over the entire fluid surface. Thermal imaging showed that temperature fields are not homogeneous in both radial and azimuthal directions. According to our estimations, the inaccuracy of thermocouple data does not exceed 5 %.

### 3. Results

The heat flux in the central part of the bottom initiates the intensive upward motion above the heater. The warm fluid cools at the free surface and moves toward the periphery, where the cooled fluid moves downward along the side wall. A large-scale advective flow occupies the whole vessel. The scheme of the basic flow is presented in figure 2. The mean advective flow consists of a convergent flow in the lower part of the vessel (1) and a divergent flow in the upper layer (2).

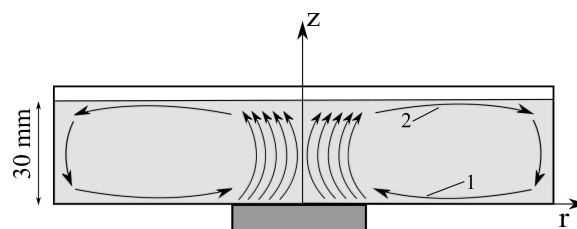


**Figure 2.** Large-scale circulation: 1 - convergent flow, 2 - divergent flow.

The convergent flow in the lower part of the layer leads to the formation of a boundary layer with potentially unstable temperature stratification above the heater and makes possible the generation of secondary convective flows. Examples of the experimental temperature profiles for different values of  $Ra$  are presented in figure 3.

The formation of secondary structures was described in detail in [5], where the structure and dynamics of secondary flows were found to be strongly dependent on heating intensity. Visualization of the secondary structures over the heater by the shadowgraph method is shown

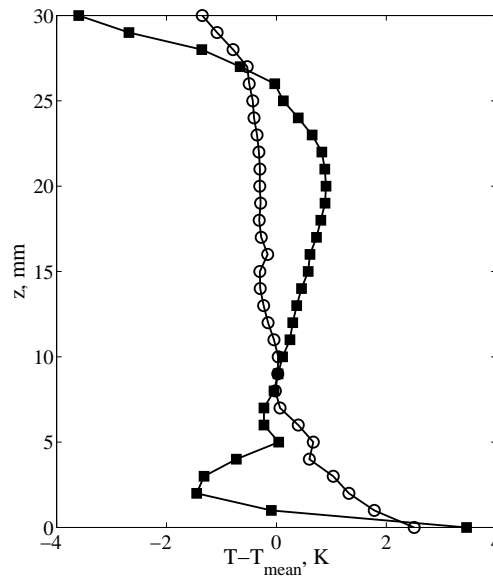


**Figure 3.** Temperature profiles at  $r = 3$  cm for  $Ra = 0.9 \cdot 10^6$  (open circles) and  $Ra = 4 \cdot 10^6$  (black squares).

in figure 4. Weak heating regimes (figure 4 a) are characterized by the appearance of ring-like rolls. An increase of the heat flux leads to more complex convective patterns - the superposition of a spiral and a system of radial rolls on the periphery (figure 4 b).

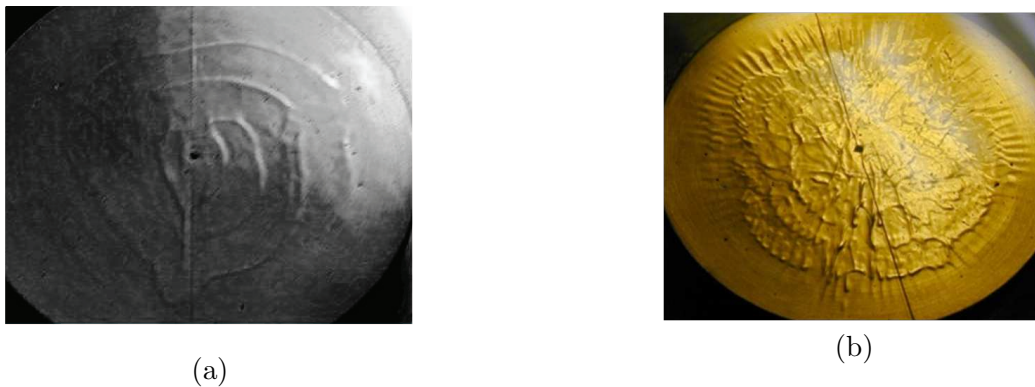


**Figure 4.** Visualization of secondary flows with shadowgraph method: (a)  $Ra = 3.3 \cdot 10^5$ , (b)  $Ra = 3.1 \cdot 10^6$

Velocity measurements given in [5] showed that radial rolls are robust and stationary. Ring-like rolls and spirals are oriented in transverse direction to the main flow and appear periodically on the heater periphery. Dependence of frequency  $F$  for transverse roll formation on the Rayleigh number for different fluids is presented in figure 5. The plot is done in a log-log scale and shows that  $F$  varies as  $F \propto Ra^{0.60}$ . This fit is shown by a solid line.

The secondary flows are responsible for intensive mixing in the boundary layer, and the variation of the secondary flow structure can lead to the change of heat transfer intensity. The dependence of  $Nu$  on  $Ra$  is shown in figure 5 b. The heat transfer grows as  $Nu \propto Ra^{0.28}$  (solid line).

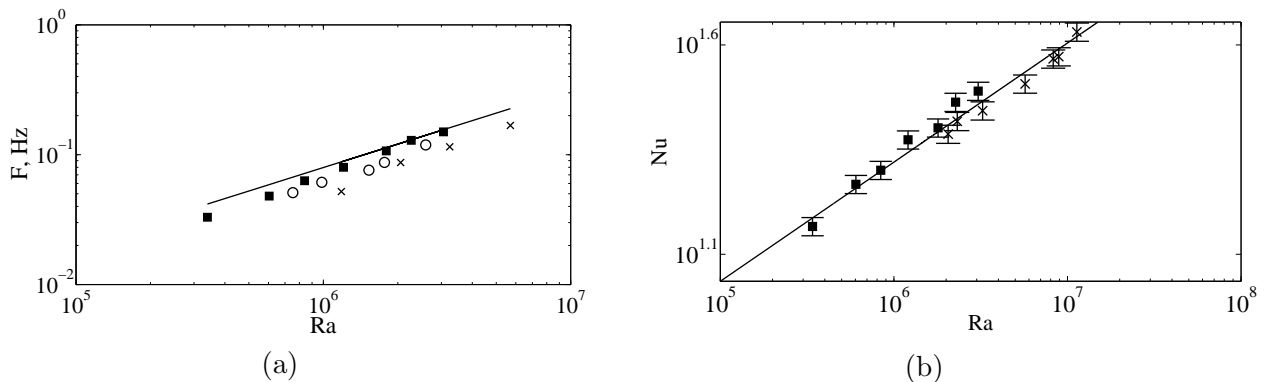


**Figure 5.** Characteristic frequency  $f$  (a) and Nusselt number (b) versus Rayleigh number for  $Pr = 209$  (black squares),  $Pr = 110$  (open circles),  $Pr = 66$  (crosses).

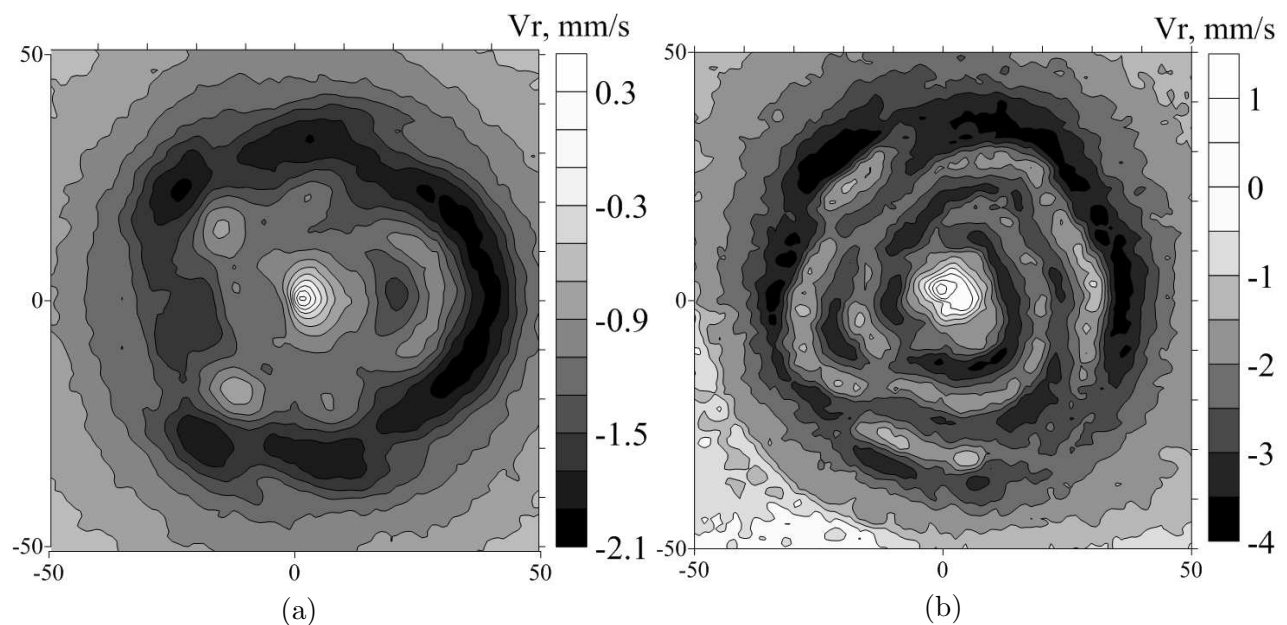


**Figure 6.** Instantaneous radial velocity fields over the heater at  $z = 3$  mm for  $Ra = 1.2 \cdot 10^6$  (a) and  $Ra = 2.9 \cdot 10^6$  (b)

We expected a more pronounced dependence of  $Nu$  on the intensity and structure of rolls. In figure 6, the instantaneous fields of radial velocity over the heater at  $z = 3$  mm are presented. The fields were obtained experimentally for  $Ra = 1.2 \cdot 10^6$  (figure 6 a) and  $Ra = 2.9 \cdot 10^6$  (figure 6 b). One can see that the form of transverse rolls changed noticeably and the value of velocity increased. However the heat transfer expressed by the Nusselt number weakly responded to it. The Nusselt numbers for these regimes are approximately equal to 22.2 ( $Ra = 1.2 \cdot 10^6$ ) and 29.4 ( $Ra = 2.9 \cdot 10^6$ ). Using the temperature measurement from the thermocouple array, the mean radial flow velocity was estimated. Figure 7 shows the dependence of the mean velocity  $V$  of convergent flow on  $Ra$ . There is almost linear dependence of  $V$  on  $Ra$  so that heat transfer for the described regimes depends mainly on the basic flow velocity.

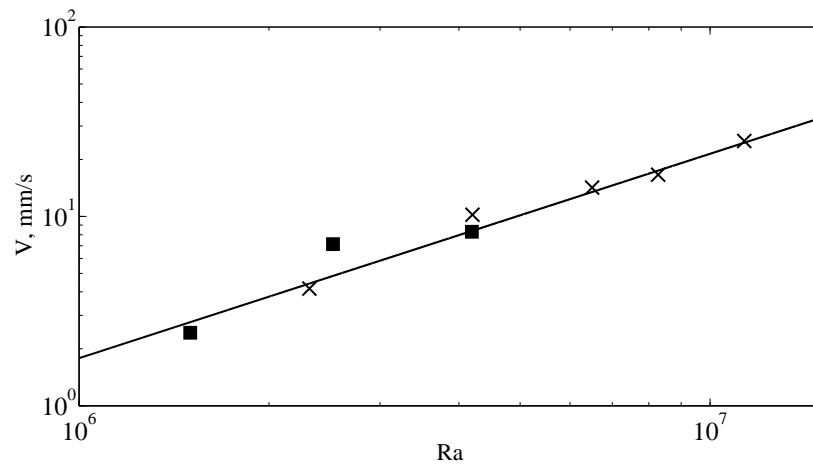


**Figure 7.** Dependence of mean radial flow velocity  $V$  on  $Ra$  for  $Pr = 209$  (black squares),  $Pr = 66$  (crosses).

#### 4. Conclusions

Heat transfer from the localized heat source in a cylindrical layer was studied experimentally for fluids with different values of kinematic viscosity and heat flux. The flow in such a system consists of large-scale advective circulation and secondary structures appeared in the thermal boundary layer above the heated area. Our temperature measurements showed that the form and intensity of secondary flows do not cause any substantial changes in the dependence of heat transfer on the Rayleigh number. It has been also shown that the mean velocity of the convergent flow has almost linear dependence on the Rayleigh number. Hence it can be concluded that for the regimes under consideration the heat transfer is predominantly dependent on the large-scale flow intensity.

#### Acknowledgments

The financial support of the grant RFBR 16-31-00150 is gratefully acknowledged.

#### References

- [1] Grossmann S and Lohse D 2008 *Phys. Rev. Lett.* **86** 3316
- [2] Aydin O and Wen-Jei Y 2000 *Int. J. Numer. Methods Heat Fluid Flow* **10** 518-529
- [3] Sharma A et al 2007 *Int. J. Therm. Sci.* **46**(12) 1232-1241
- [4] Sezai I and Mohamad A 2000 *Int. J. Heat Mass Transfer* **43**(13) 2257-2266
- [5] Sukhanovskii et al. 2016 *Physica D* **316** 23-33
- [6] Maughan JR and Incropera FP 1990 *Int. J. Heat Mass Transf.* **33** 555
- [7] Chiu WKS. et al 2000 *Phys. Fluids* **12** 2128
- [8] Benderradji A et al 2008 *Heat Mass Transfer* **44** 1465
- [9] Sukhanovsky et al. 2012 *Eur. Phys. J. B* **85** 12